2012

Structural and magnetic properties of Mn$_{2+\delta}$TiSn

Parashu Kharel
University of Nebraska-Lincoln, pkharel2@unl.edu

Yung Huh
University of Nebraska-Lincoln, yung.huh@sdstate.edu

Shah R. Valloppilly
University of Nebraska-Lincoln, svalloppilly2@unl.edu

Xingzhong Li
University of Nebraska-Lincoln, xli2@unl.edu

N. Al-Agtash
University of Nebraska at Omaha

See next page for additional authors

Kharel, Parashu; Huh, Yung; Valloppilly, Shah R.; Li, Xingzhong; Al-Agtash, N.; Tarawneh, K.; Krage, E. S.; Sabirianov, Renat F.; Skomski, Ralph; and Sellmyer, David J., "Structural and magnetic properties of Mn$_{2}$ $_{+\delta}$TiSn" (2012). *David Sellmyer Publications*. 228.
https://digitalcommons.unl.edu/physicssellmyer/228

Authors

Parashu Kharel, Yung Huh, Shah R. Valloppilly, Xingzhong Li, N. Al-Agtash, K. Tarawneh, E. S. Krage, Renat F. Sabirianov, Ralph Skomski, and David J. Sellmyer

Structural and magnetic properties of Mn$_{2+\delta}$TiSn

P. Kharel,[1,2,a)] Y. Huh,[2,3] V. R. Shah,[2] X. Z. Li,[2] N. Al-Aqtash,[4] K. Tarawneh,[5] E. S. Krage,[2,3]
R. F. Sabirianov,[2,4] R. Skomski,[1,2] and D. J. Sellmyer[1,2]

[1]*Department of Physics and Astronomy, University of Nebraska, Lincoln, Nebraska, 68588, USA*
[2]*Nebraska Center for Materials and Nanoscience, University of Nebraska, Lincoln, Nebraska, 68588, USA*
[3]*Department of Physics, South Dakota State University, Brookings, South Dakota, 57007, USA*
[4]*Department of Physics and Astronomy University of Nebraska, Omaha, Nebraska, 68182, USA*
[5]*Department of Science and Humanities, Princes Sumaya University for Technology (PSUT) Amman, Jordan*

The structural and magnetic properties of Mn$_{2+\delta}$TiSn prepared by arc melting and annealing have been investigated. Structural studies show that the compound crystallizes in the hexagonal Ni$_3$Sn-type structure with $a = 5.70$ Å and $c = 4.55$ Å. The phase stability of Mn$_2$TiSn in the hexagonal structure is supported by the first-principle electronic structure calculations where the total energy per unit-cell volume in the hexagonal structure is smaller than that in the cubic structure. Field and temperature dependence of magnetization show that the sample is magnetically ordered with a Curie temperature around 400 K. The anisotropy energy calculated from the high-field data is 4.0×10^5 ergs/cm^3 at 300 K but increases by a factor of two (8.6×10^5 ergs/cm^3) as temperature decreases to 10 K. The observed magnetic properties are explained as the consequences of competing ferromagnetic and antiferromagnetic interactions between different magnetic sublattices. © *2012 American Institute of Physics.* [doi:10.1063/1.3672395]

Magnetically ordered X_nYZ (X,Y = transition metals, Z = main group element; $n = 1$ or 2) Heusler compounds with high-spin polarization and Curie temperature well above room temperature have drawn much attention because of their potential for spintronic applications.[1] A ternary intermetallic compound Mn$_2$TiSn is one of such compounds predicted to be nearly half metallic with spin polarization of 97% and ferrimagnetic with Curie temperature above room temperature (354 K).[2] Although there are few reports on the isostructural compounds Co$_2$TiSn[3] and Fe$_2$TiSn,[4] no reports of experimental work on Mn$_2$TiSn have been found to date. Mn$_2$TiSn is of particular interest because the number of valence electrons (22) in this material is the same as that of the prototypical half-metallic ferromagnet NiMnSb.[5] This equality in valence electron count is important as the structural stability and the physical properties of Heusler compounds are strongly dependent on the number of valence electrons.[6] Usually, X_2YZ Heusler compounds crystallize in the $L2_1$ cubic structure (space group ($Fm\bar{3}m$)), but compounds with tetragonal distortion have also been found.[7] Here we present the synthesis and characterization of a compound with elemental composition close to X_2YZ (Mn$_{2+\delta}$TiSn; $0 < \delta < 0.5$). We find that the crystal structure of the synthesized alloy is hexagonal $D0_{19}$ similar to that of Mn$_3$Sn and is different from that of prototype X_2YZ Heusler compound. The phase stability of the Mn$_2$TiSn in the hexagonal structure is also supported by our first-principle electronic structure calculations.

Mn$_{2+\delta}$TiSn powder samples were prepared by arc melting, annealing, and grinding. The Mn$_{2+\delta}$TiSn ingot was prepared by arc melting Mn, Ti, and Sn on a water-cooled Cu hearth in a highly pure argon environment. The intended stoichiometry of the sample was obtained based on the weight of the constituent metals. We used excess Mn in the starting material to compensate the loss during arc melting. The ingot was melted several times to improve homogeneity and then annealed at 600 °C for 65 h in a tubular vacuum furnace. A pressure of 10^{-6} Torr was maintained during annealing. The annealed ingot was crushed into fine powder, which was used to study the structural and magnetic properties.

Figure 1(a) shows the room-temperature x-ray diffraction (XRD) pattern of Mn$_{2+\delta}$TiSn powder sample. To identify the phase and crystal structure of the sample, we simulated powder x-ray diffraction patterns corresponding to the relevant structures[8] and compared them with the experimental XRD pattern. The experimental XRD pattern both in relative intensity and peak position shows an excellent match with the simulated diffraction pattern based on Mg$_3$Cd or Ni$_3$Sn-type structure ($D0_{19}$ strukturbericht designation, space group ($P6_3/mmc$)), which is identical to the structure of the Mn$_3$Sn phase. Mn$_2$TiSn unit cell in the hexagonal structure is shown in Fig. 1(b). The lattice parameters extracted from the simulation are $a = 5.70$ Å and $c = 4.55$ Å. Although the intensities of most of the peaks in the XRD pattern match perfectly with that of the simulated pattern, the difference in the experimental and simulated intensities of (002) peak indicates the presence of small amounts of unreacted elemental impurities in the sample. We attribute this difference to the superposition of Ti (002) and Mn$_2$TiSn (002) peaks in the experimental pattern.

Figure 2 shows the selected-area electron-diffraction (SAED) pattern taken from some of the grains at the thin edge of the specimen prepared from the Mn$_{2+\delta}$TiSn powder sample. The region where the SAED pattern was recorded is
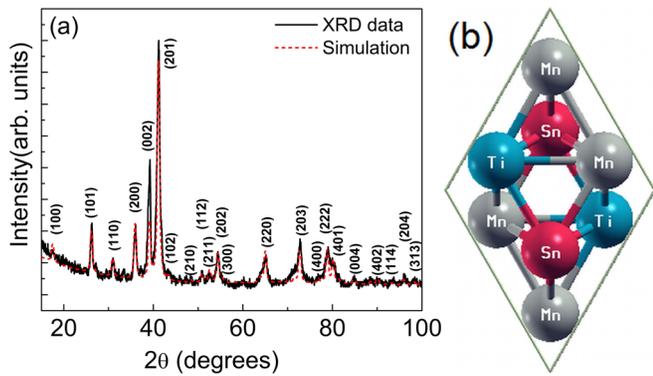
a)Electronic mail: pkharel2@unl.edu.

FIG. 1. (Color online) (a) Xray diffraction pattern of the $Mn_{2+\delta}TiSn$ power sample recorded at room temperature (solid line) and the simulated pattern for hexagonal Ni_3Sn-type structure (dotted line). (b) Mn_2TiSn unit cell in the hexagonal $D0_{19}$ structure.

shown in the bright field image of the specimen (see the inset of Fig. 2). The SAED pattern indicates that our $Mn_{2+\delta}TiSn$ compound has a hexagonal Ni_3Sn-type crystal structure, which is consistent with the XRD result. The elemental composition of the compound determined from the TEM/EDX analysis of the small selected area is $Mn_{2.1}TiSn$, which is close to Mn_2TiSn. However, a similar scan over larger areas in SEM/EDX shows more Mn, where the elemental composition is $Mn_{2.4}TiSn$.

Figure 3 shows the field dependence of magnetization at 300 K and also at 10 K. At room temperature, the sample has a coercivity (H_c) of about 1 kOe, which increases substantially at low temperatures (2.4 kOe at 10 K). At 10 K, as shown in the inset (a) of Fig. 3, the magnetization shows a small jump as the field passes through zero. As we have mentioned above, the sample may contain elemental impurities including Mn, which probably form small clusters with some uncompensated spins. We believe that the kinks observed in the low-temperature $M(H)$ loops are caused by the magnetization reversal of these uncompensated spins as the field changes direction. Although the magnetization shows an approach to saturation, it does not fully saturate even at 6 T. The room-temperature magnetization at 6 T is 9.3 emu/g, which increases with decreasing temperature and reaches 15.8 emu/g at 10 K. The lack of high-field saturation
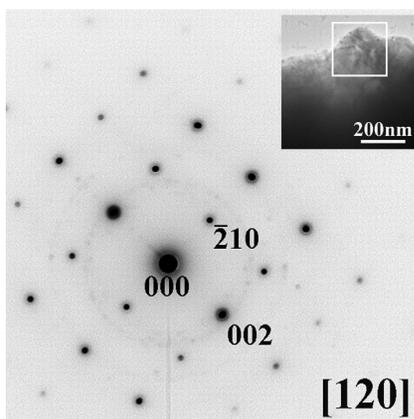

FIG. 2. Selected area electron diffraction (SAED) pattern taken from a specimen of $Mn_{2+\delta}TiSn$ powder sample. The pattern was taken from several grains of the region indicated by a square in the bright field image as shown in the inset.
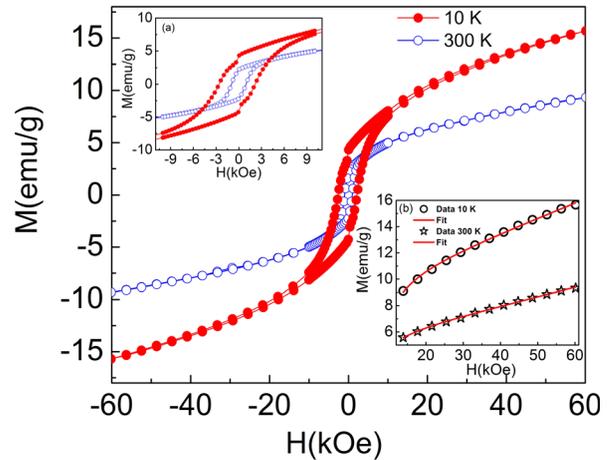

FIG. 3. (Color online) Magnetization as a function of magnetic field $M(H)$ for $Mn_{2+\delta}TiSn$ samples at 10 K and 300 K. Inset (a) shows the close-up view of the $M(H)$ loops near the coercive field. The high-field magnetization data fitted to the equation $M = M_0 (1 - A/H^2) + \chi H$ are shown as the solid lines in inset (b).

of $M(H)$ suggests that $Mn_{2+\delta}TiSn$ has a substantial value of magnetic anisotropy K. We have calculated the anisotropy constant K from the high-field magnetization data using $M = M_0 (1 - A/H^2) + \chi H$; $A = 4 K^2/15M_0^2$, where M_0 is spontaneous magnetization, A is a constant that depends on K, and χ is the high-field susceptibility.[9] The values of M_0, A, and χ were obtained from the best fit of the data to the above equation (see inset (b) of Fig. 3). The values of K determined from the fit are 4.0×10^5 ergs/cm^3 and 8.6×10^5 ergs/cm^3 at 300 K and 10 K, respectively. The coercivity has also increased by the same ratio as the anisotropy (by a factor of 2) in this temperature range, although the actual mechanism giving rise to coercivity is not clear. These values of K are comparable to the values reported for other Heusler alloy films such as Co_2FeAl.[10]

The temperature dependence of magnetizations at magnetic fields 100 Oe, 500 Oe, and 1000 Oe are shown in Fig. 4. Interestingly, the magnetization can be described well with the simple equation $M(T) = M_0[(1 - p)\{1 - B(T/T_c)^{3/2}\} + p(1 - T/T_c)^{1/2}]$. The first part of this heuristic interpolation formula describes the spin-wave behavior, and the second part characterizes the mean-field critical-point behavior near the Curie point.[11] The parameters M_0, $p = (T/T_c)^n$, B, and T_c are the spontaneous magnetization, a weight factor, spin-wave stiffness constant, and the Curie temperature, respectively. The Curie temperature determined from the best fit of the 100 Oe M(T) data to the above equation is 405 K. This is slightly higher than the value (354 K) predicted for Mn_2TiSn in the hypothetical $L2_1$ structure from theoretical calculations.[2] In low magnetic fields (100 Oe), there is a clear splitting between the zero field-cooled (ZFC) and field-cooled (FC) data below the Curie temperature. The divergence between the ZFC and FC curves increases with decreasing temperature, but the ZFC curve passes through a maximum near 60 K. The splitting between the ZFC and FC curves suggests that the sample contains magnetically inhomogeneous states.[12] A possible explanation is that the competing ferromagnetic and antiferromagnetic interactions between different Mn sublattices may lead to a ferrimagnetic state giving rise to the splitting in ZFC and FC curves. The anomaly in 100 Oe ZFC data near 60 K can be
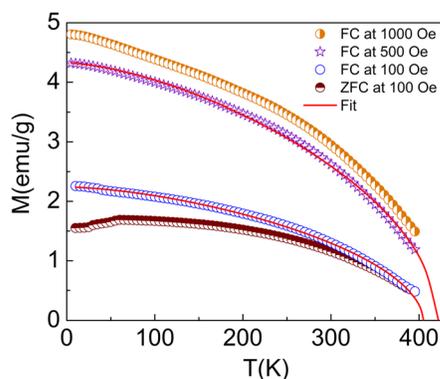
FIG. 4. (Color online) Temperature dependence of magnetization at magnetic fields 100 Oe, 500 Oe, and 1000 Oe. For the 100-Oe measurement, both zero-field cooled (ZFC) and field-cooled (FC) data are shown. The solid lines are the fits to the equation $M(T) = M_0[(1-p)\{1 - B(T/T_c)^{3/2}\} + p(1 - T/T_c)^{1/2}]$.

FIG. 5. (Color online) Total energy as a function of unit cell volume per formula unit for Mn_2TiSn.

attributed to the random freezing of the magnetic moments into various metastable states.

To understand the observed structural and magnetic properties of $Mn_{2+\delta}TiSn$ alloy and to analyze the relative phase stability of Mn_2TiSn in $L2_1$ cubic and $D0_{19}$ hexagonal structures, we performed first-principle total energy calculations using the projector-augmented wave method,[13,14] within a Perdew-Burke-Ernzerhof generalized gradient approximation[15] of the density functional theory. The simulations were performed using periodic boundary conditions. We used $12 \times 12 \times 12$ k-point sampling, and positions of atoms in the unit cell were relaxed using the Hellmann-Feynman scheme until forces were less than 0.003 eV/Å.

We considered two ordered hexagonal Mn_2TiSn structures: one with Ti atoms as the nearest neighbors and the other with Ti atoms as the second-nearest neighbors. The relaxed atomic positions are almost unchanged in the case of Ti as the nearest neighbors (c/a has increased slightly), while the Wyckoff's internal x value reduced slightly to $x = 0.81$ in the case of Ti as the second nearest neighbors. We have found that the hexagonal structure with Ti atoms as the nearest neighbors has a higher total energy than that of the hexagonal structure with Ti atoms as the second-nearest neighbors. On the other hand, as shown in Fig. 5, the $D0_{19}$ hexagonal structure with Ti as the second nearest neighbor has lower total energy than that of the corresponding $L2_1$ cubic structure. We have also estimated the exchange coupling in the above-mentioned two cases of hexagonal Mn_2TiSn structures. In both cases, Ti presence induces ferromagnetic (FM) coupling between Mn atoms where the energy of FM state is lower by 0.24 eV/f.u. than that of the antiferromagnetic (AFM) state. The magnetic moment in the ordered state with Ti as the second nearest neighbor where Mn−Mn interaction is FM, is 3.5 μ_B/f.u. In this case, the overall magnetic state is ferrimagnetic because Mn ($m = 2.3 \mu_B$) and Ti ($m = -0.79 \mu_B$) are anti-aligned. However, the experimental value of high-field magnetization at 10 K ($\sim 0.8 \mu_B$/f.u) is much smaller than the value obtained from the calculation. This suggests that the distribution of Ti in the $Mn_{2+\delta}TiSn$ sample is not uniform and the antiferromagnetic interaction between Mn atoms is expected in the
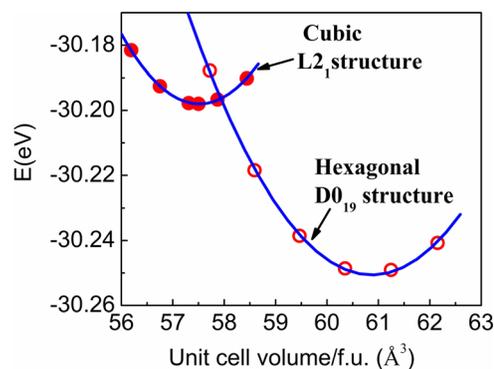
Mn-rich areas. The calculated degree of spin polarization in the hexagonal structure is only 41%, which is much lower than the value (97%) reported for the cubic structure.[2]

In conclusion, we have prepared $Mn_{2+\delta}TiSn$ powder samples using arc melting and annealing. The samples have crystallized in the hexagonal Ni_3Sn-type structure and are magnetically long-range ordered with the Curie temperature well above room temperature. *Ab initio* total-energy calculations show that the $D0_{19}$ hexagonal Ni_3Sn-type structure is more stable than the $L2_1$ cubic structure. The observed magnetic properties are consistent with the presence of ferrimagnetic order in the sample, but the magnetic structure seems to be more complex than the one considered in the calculation. Because the powder sample shows substantial magnetic anisotropy, it will be useful to investigate various properties including magnetic properties and the state of spin polarization in thin films to determine the potential of this material for device applications.

[1] M. I. Katsnelson, V. Yu. Irkhin, L. Chioncel, A. I. Lichtenstein, and R. A. de Groot, Rev. Mod. Phys. **80**, 315 (2008).
[2] M. Meinert, J.-M. Schmalhorst, and G. Reiss, J. Phys.: Condens. Matter **23**, 036001 (2011).
[3] S. Majumdar, M. K. Chattopadhyay, V. K. Sharma, K. J. S. Sokhey, S. B. Roy, and P. Chaddah, Phys. Rev. B **72**, 012417 (2005).
[4] A. Ślebarski, M. B. Maple, E. J. Freeman, C. Sirvent, D. Tworuszka, M. Orzechowska, A. Jezierski, S. Chiuzbaian, and M. Neumann, Phys. Rev. B **62**, 3296 (2000).
[5] S. J. Youn and B. I. Min, Phys. Rev. B **51**, 10436 (1995).
[6] T. Graf, C. Felser, and S. P. Parkin, Prog. Solid State Chem. **39**, 1 (2011).
[7] F. Wu, S. Mizukami, D. Watanabe, H. Naganuma, M. Oogane, Y. Ando, and T. Miyazaki, Appl. Phys. Lett. **94**, 122503 (2009).
[8] W. Kraus and G. Nolze, Powder Cell, see http://www.ccp14.ac.uk/ccp/web-mirrors/powdcell/a_v/v_1/powder/e_cell.html.
[9] G. Hadjipanayis and D. J. Sellmyer, Phys. Rev. B **23**, 3349 (1981).
[10] Z. Wen, H. Sukegawa, S. Mitani, and K. Inomata, Appl. Phys. Lett. **98**, 242507 (2011).
[11] X. Guo, X. Chen, Z. Altounian, and J. O. Ström-Olsen, J. Appl. Phys. **73**, 6275 (1993).
[12] E. Duman, M. Acet, Y. Elerman, A. Elmali, and E. F. Wassermann, J. Magn. Magn. Mater. **238**, 11 (2002).
[13] P. E. Blöchl, Phys. Rev. B **94**, 17953 (1994).
[14] G. Kresse and D. Joobert, Phys. Rev. B **59**, 1758 (1999).
[15] J. P. Perdew, K. Burke, and M. Ernzerhof, Phys. Rev. Lett. **77**, 3865 (1996).